Aggregation in a mixture of Brownian and ballistic wandering particles

S. G. Alves

Departamento de Física, Universidade Federal de Minas Gerais, CP 702, 30161-970, Belo Horizonte, Minas Gerais, Brazil

S. C. Ferreira, Jr.*

Departamento de Física, Universidade Federal Viçosa, 36571-000, Viçosa, Minas Gerais, Brazil

In this paper, we analyze the scaling properties of a model that has as limiting cases the diffusion-limited aggregation (DLA) and the ballistic aggregation (BA) models. This model allows us to control the radial and angular scaling of the patterns, as well as their gap distributions. The particles added to the cluster can follow either ballistic trajectories, with probability P_{ba}, or random ones, with probability $P_{rw}=1-P_{ba}$. The patterns were characterized through several quantities, including those related to the radial and angular scaling. The fractal dimension as a function of P_{ba} continuously increases from $d_f \approx 1.72$ (DLA dimensionality) for $P_{ba}=0$ to $d_f \approx 2$ (BA dimensionality) for $P_{ba}=1$. However, the lacunarity and the active zone width exhibit a distinct behavior: they are convex functions of P_{ba} with a maximum at $P_{ba} \approx 1/2$. Through the analysis of the angular correlation function, we found that the difference between the radial and angular exponents decreases continuously with increasing P_{ba} and rapidly vanishes for $P_{ba} > 1/2$, in agreement with recent results concerning the asymptotic scaling of DLA clusters.

PACS number(s): 61.43.Hv, 05.40.Fb, 47.53.+n, 47.54.−r

I. INTRODUCTION

Nonequilibrium growth models of clusters of identical particles have attracted a lot of attention in the past two decades [1,2]. Certainly, the most studied one is the diffusion-limited aggregation (DLA) model proposed by Witten and Sander [3] for the modeling of metal particle aggregation. In spite of its simplicity, this model is a noteworthy example in which a very simple algorithm generates disordered patterns with nontrivial scaling [4–7]. In the DLA model, the particles are released at points distant from the cluster and follow random walks of unitary steps, which are stopped when these particles contact the cluster and irreversibly aggregate to it. Another important aggregation model with nontrivial scaling is the ballistic aggregation (BA) [8,9], in which ballistic trajectories at random directions replace the random walks characteristic of the DLA model. Differently from the DLA case, the patterns generated by the BA model are asymptotically homogeneous (fractal dimension equal to the space dimension), but this asymptotic regime is characterized by a power law approach [9,10].

Several generalized versions of the DLA model were proposed [1], including those concerned with the transition between DLA and BA models [10–12]. In a recent work, Ferreira *et al.* [10] built a model in which the particles follow random trajectories with drifts at random directions. The bias is controlled by a parameter λ that, when varied, leads the model from BA (λ=0) to DLA (λ=1). The clusters are asymptotically nonfractal (exhibiting the BA-like scaling with fractal dimension $d_f=2$) for any λ ≠ 1, but following a DLA-like scaling ($d_f \approx 1.71$) for short length scales. Using the concept of scaling functions, these ideas can be summarized as

$$M(l) = l^{d_{DLA}} f(l/\xi), \tag{1}$$

in which

$$f(x) \sim \begin{cases} \text{const} & \text{if } x \ll 1 \\ x^{d-d_{DLA}} & \text{if } x \gg 1. \end{cases} \tag{2}$$

In these equations, l is the size of the cluster, d is the space dimension, d_{DLA} is the DLA fractal dimension, and ξ is the characteristic crossover radius from DLA- to BA-like scaling regimes. The last diverges as $\xi \sim |1-\lambda|^{-\nu}$, where $\nu = 0.61 \pm 0.01$. This transition between DLA and BA regimes was introduced by Meakin [13] in an early generalization of the DLA model. This model is very similar to that analyzed by Ferreira *et al.* [10]. The main difference is that the drift of all trajectories is fixed at a lattice direction in Meakin's model, in which, along the trajectory, the particle is moved one step in the drift direction with probability P, or moves at random to one of its four nearest-neighbor sites with probability $1-P$. The model generates patterns with a growth tendency along the opposite direction of the drift. In this work, Meakin argued that the crossover radius scales as $\xi = P^{-1}$ while Nagatani [14], through a real-space renormalization-group approach, found $\xi \sim P^{-1/(d-d_f)}$.

Early studies indicated that the DLA aggregates exhibit distinct scaling exponents for radial and angular correlations. The two-point correlation function Γ, which gives the probability to find a particle at a distance between r and $r+\delta r$, $\delta r \ll r$, from another particle, is given by [1]

$$\Gamma(r) \sim r^{-\alpha_r}, \tag{3}$$

where $\alpha_r = d - d_f$. For off-lattice DLA, the exponent found was $\alpha_r \approx 0.29$. In turn, the angular correlation function Φ_R, which gives the probability to find two particles with angular separation θ measured in relation to the origin at a distance R, follows a power law decay for small θ,

*Email address: silviojr@ufv.br

$$\Phi_R(\theta) \sim \theta^{-\alpha_\theta}. \qquad (4)$$

For uniform self-similar fractals $\alpha_r = \alpha_\theta$, but this was not observed for the DLA model, for which $\alpha_\theta \approx 0.41$ [15].

In this work, we used careful simulations to analyze the transition between DLA- and BA-like regimes in a model where both random and ballistic trajectories are included. Differently from the previously described models [10,13], the trajectories are not characterized by distinct behaviors at short (random) and large (ballistic) scales. Indeed, we are interested in the scaling of clusters grown from a mixture of particles, which can follow either ballistic or random trajectories. The paper outline is the following. In Sec. II, the algorithm and the computer implementations are described. In Sec. III, the quantities describing the scaling of the cluster are introduced and the corresponding results discussed. Finally, we summarize the results of the paper in Sec. IV.

II. MODEL AND COMPUTER IMPLEMENTATION

The present model is concerned with the aggregation of particles which can follow either ballistic or random trajectories. Notice that there are two kinds of independent trajectories, which do not exhibit both random and ballistic components simultaneously, as those used in Ref. [10]. Two-dimensional off-lattice simulations starting from a single particle of unitary radius stuck to the origin were considered. The model's rules are very simple. For each time step, a kind of trajectory, Brownian or ballistic, is chosen with probabilities P_{rw} and P_{ba}, respectively. Then, particles are launched one at a time using the selected rule until one of them sticks to the cluster. Notice that in these rules we are taking into account only the particles that are added to the cluster and not those that get too far from the cluster and are excluded.

The particles are released at a launching circle of radius $r_l > r_{max}$ centered at the origin, where r_{max} is the largest distance from the origin among all the aggregated particles. As in the off-lattice DLA model [18], the cluster grows when a walker contacts any particle of the aggregate and sticks to the corresponding position. Also, if the walker crosses a killing circle of radius $r_k > r_l$ centered at the origin, it is discarded and a second one is released at a new random point on the launching circle. The previously introduced variables (r_l and r_k) should be as large as possible. However, computational limitations restrict their values. For the sake of convenience, we introduce a new variable δ by the definition $r_l = r_{max} + \delta$. The choices of δ and r_k depend on the kind of trajectory. For random walks, r_l can be a few particle diameters larger than r_{max}, whereas r_k must be very large [1]. Consequently, we used $\delta = 5$ and $r_k = 100 r_{max}$. For ballistic trajectories, undesirable shadow effects are reduced as r_l increases [19,20]. Thus, we used $\delta = 100 r_{max} + 800$. Finally, ballistic trajectories which cross the launching circle cannot turn back inside the circle, and so we chose $r_k = r_l + 2$.

Large-scale off-lattice simulations with rigorous statistical sampling require very efficient algorithms. First, it is necessary to improve the efficiency of the routines for the trajectories. In the case of random walks, we used a standard method, in which particles outside the launching circle take
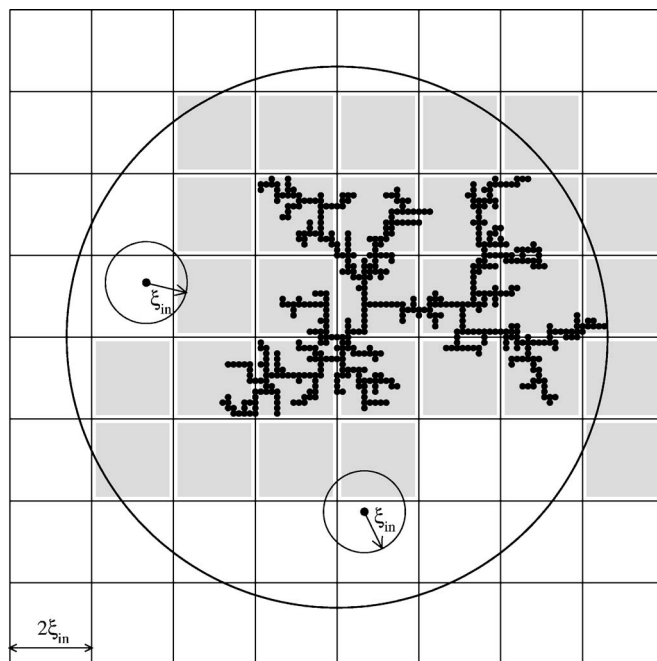

FIG. 1. Schematic representation of the "optimized random trajectories." We show a DLA aggregate and a mesh of cells $2\xi_{in} \times 2\xi_{in}$. Long steps are forbidden in the gray boxes and allowed in the white ones. Also, two long steps are illustrated.

long steps ξ_{out} if these steps do not bring up a particle inside the launching circle. An adequate choice is $\xi_{out} = \max(r - r_{max} - 5, 1)$, where r is the distance of the walker from the origin. Also, in the inner region of the circle delimiting the cluster there are large empty regions. So, we adopted an algorithm like those used by Ball and Brady [21], in which particles inside the launching circle can take a long step of length ξ_{in} if they cannot cross any part of the aggregate along this long step.

An efficient determination of ξ_{in} is decisive in order to guarantee the success of the procedure. In order to accomplish this, we define a coarse-grained mesh with cells of size $2\xi_{in} \times 2\xi_{in}$ as illustrated in Fig. 1. The boxes depicted in gray are those in which the random walk could reach the cluster after a step of length ξ_{in} and, consequently, a long step is forbidden. In this case, we have two options: the particle executes a unitary step or tries a shorter step of length ξ'_{in}, where $1 < \xi'_{in} < \xi_{in}$, using another auxiliary coarse-grained mesh. Indeed, we can use several auxiliary meshes in order to maximize the algorithm efficiency. In this work, three values, $\xi_{in} = 8$, 16, and 32, were used. Through this procedure, large simulations become up to two orders of magnitude faster than those using only long steps outside the launching circle.

Finally, an efficient search mechanism for determining when the walker does or does not have a contact with the aggregate is indispensable. We used two procedures for this task. In the first one, the particle positions are mapped on a square lattice by the approximation of their real coordinates to the nearest integer, producing an on-lattice auxiliary cluster. So, the verification of the contact is done only if the particle is inside a nearest or a next-nearest empty site neigh-
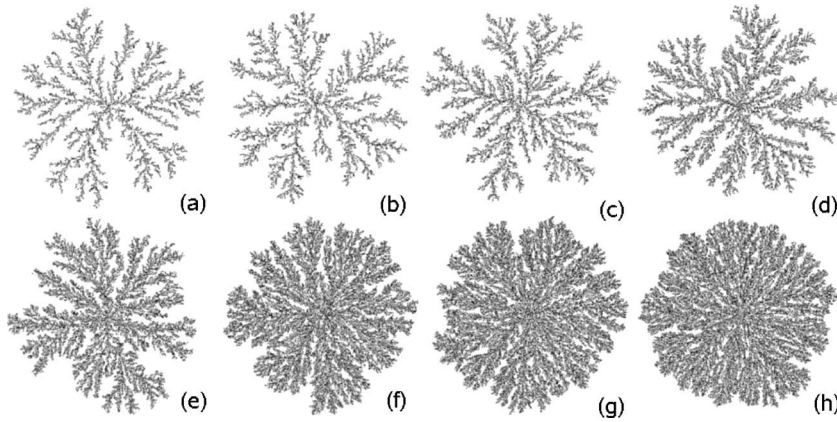
FIG. 2. Growth patterns for distinct values of the parameter P_{ba}: (a) 0.1, (b) 0.3, (c) 0.5, (d) 0.7, (e) 0.9, (f) 0.95, and (h) 0.99. All simulations are stopped when the cluster reaches the border of a region 750×750 centered at the origin. The number of particles varies from $N \simeq 3 \times 10^4$ ($P_{ba} = 0.1$) to $N \simeq 1.6 \times 10^5$ ($P_{ba} = 0.99$).

boring the on-lattice auxiliary cluster. In the second optimization procedure, a coarse-grained mesh of 8×8 cells was used to limit the verification on a region near the walker position.

III. RADIAL AND ANGULAR SCALING

The model exhibits a smooth transition from DLA to BA-like growth patterns as the parameter P_{ba} varies from 0 to 1. In Fig. 2, in which growth patterns for distinct probabilities P_{ba} are shown, one can observe clusters that are qualitatively very similar to the DLA aggregates for $P_{ba} \lesssim 0.5$, whereas BA-like clusters are observed for $P_{ba} \gtrsim 0.95$. These patterns were grown until a part of them reaches the edge of a region of size $L \times L$, where $L = 750$. Notice that $P_{ba} = 0.5$ is an important case, in which half of the particles were grown using the DLA model and the another half were grown using the BA model.

The scaling properties of the clusters were characterized by the radial and angular distributions of the particles, as well as the size of their active (growing) zone. We grew 2D off-clusters limited by a region of size $10^4 \times 10^4$. Again, the simulations were stopped when the cluster reaches the border of this region. The radial scaling was characterized by the fractal dimension and the lacunarity [1]. The fractal dimension d_f and the lacunarity A were determined using the mass-radius and the radius of gyration methods. The mass-radius method consists of counting the number of particles M in a hypersphere of radius r centered at the origin. We expect a power law relation for self-similar clusters,

$$M(r) = A_m r^{d_f}, \tag{5}$$

where the amplitude A_m is a measure of the lacunarity. To be more precise, the DLA clusters are characterized by a multi-scaling, which leads to a slow convergence to the asymptotic scaling exponents. However, large-scale simulations confirm that these clusters are asymptotically fractal. For details, see Refs. [1,22]. The radius of gyration r_g is defined as

$$r_g = \left(\frac{1}{N} \sum_{i=1}^{N} r_i^2 \right)^{1/2}, \tag{6}$$

where r_i is the distance from the origin of the ith aggregated particle and N the total number of particles in the cluster. The

gyration radius scales with the number of particles as

$$r_g = BN^\nu, \tag{7}$$

where $\nu = 1/d_f$ and B can be related to the lacunarity through the relation

$$A_g = \frac{1}{B^{1/\nu}}. \tag{8}$$

Notice that $A_m \neq A_g$ since their definitions are different. But they exhibit the same qualitative behavior because $A_m \propto A_g$.

In Fig. 3(a), the double logarithm plots of the curves $M(r)$ against r are shown for several P_{ba} values. The slope continuously increases from $d_f = 1.723 \pm 0.007$ for $P_{ba} = 0.10$ (a value close to the well-known DLA fractal dimension $d_f = 1.715 \pm 0.004$ [18]) toward 2.0 as P_{ba} increases, as can be seen in Fig. 3(b), in which the fractal dimension is plotted as a function of P_{ba}. Remarkably, instead of the qualitative behavior observed for the fractal dimension (an increasing function of P_{ba}), the lacunarity is a convex function of P_{ba} with a maximum at $P_{ba} \approx 1/2$, as shown in the inset of Fig. 3(a). These results show that if the number of DLA particles is larger than the number of BA ones, an increasing P_{ba} produces patterns with more dense branches (larger d_f values) but with larger empty regions (larger lacunarity). However, when the number of BA particles exceeds the number of DLA ones, the width of the branches increases while the size of the empty regions decreases with P_{ba}. An explanation for such a behavior can be obtained from the active zone analysis described next.

We define the active zone as the fraction f of the latest particles added to the cluster, and its width σ_f as the standard deviation of the distances from the origin of these particles. So,

$$\sigma_f^2 = \frac{1}{fN} \sum_{i=N_f}^{N} (r_i - \langle r \rangle)^2, \tag{9}$$

where $N_f = (1-f)N$ and

$$\langle r \rangle = \frac{1}{fN} \sum_{i=N_f}^{N} r_i. \tag{10}$$

In all simulations, we used $f = 0.1$. In Fig. 4, the width of the active zone as a function of the number of particles is
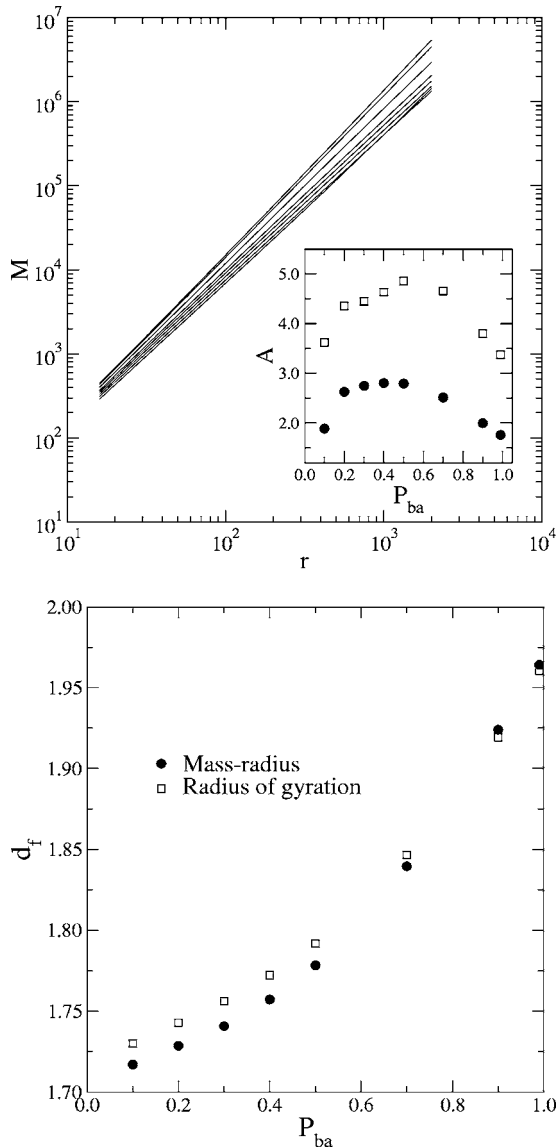
FIG. 4. Active zone width σ as a function of the number of particles for $P_{ba}=0.20$ (●) and 0.90 (○). The straight lines correspond to power law fits. In the inset, we show σ as a function of P_{ba} for a mean active zone radius $r \approx 340$. The line is a cubic fit used as a guide to the eyes. For these simulations, we used clusters of size $L=10^4$ and averages were done over 10^3 independent samples.

FIG. 3. (a) Mass against radius for distinct P_{ba} values: 0.10, 0.20, 0.30, 0.40, 0.50, 0.70, 0.90, and 0.99 from the bottom to the top. (b) Fractal dimension as a function of P_{ba} determined from the mass-radius (●) and gyration-radius (□) methods. In the inset, we show the lacunarity as a function of P_{ba} obtained from mass-radius (●) and radius of gyration (□) methods. For these simulations, we used clusters of size $L=10^4$ and averages done over 10^3 independent samples. The number of particles in these clusters varies from 7×10^6 for $P_{ba}=0.1$ to 3×10^7 for $P_{ba}=0.99$.

shown for two distinct P_{ba} values. For $P_{ba}<0.5$, the simulations indicate that there is a single power law regime $\sigma \sim N^\zeta$ while a crossover between two power laws $\sigma \sim N^{\zeta'}$ for small length scales and $\sigma \sim N^\zeta$ for large ones is observed for $P_{ba} \gtrsim 0.5$. In the asymptotic regime ($N \to \infty$), the exponent $\zeta \to \nu$ for $p<1$ as observed in the DLA model [18]. For $P_{ba} \gtrsim 0.5$, we found $\zeta' \approx 0.46$, 0.42, and 0.36 for $P_{ba}=0.5$, 0.7, and 0.9, respectively. Indeed, our simulation suggests that $\zeta' \to 0.33$ as $P_{ba} \to 1$, in agreement with the statement that interface scaling of the BA belongs to the Kardar-Parisi-Zhang universality class [23]. To be more precise, the inter-
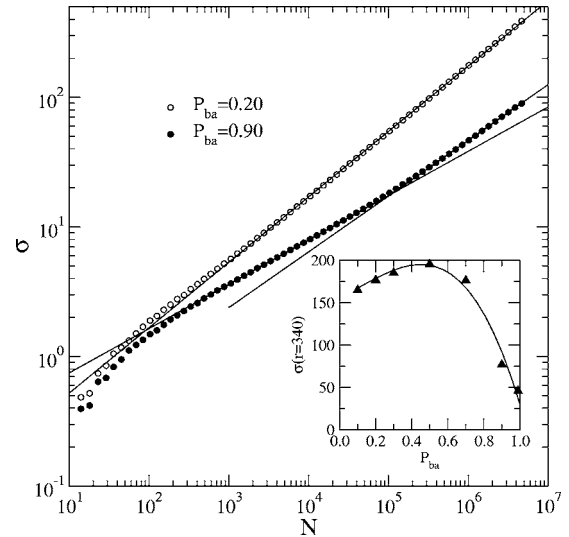
face scaling of ballistic deposition models was widely studied and rigorous simulations confirmed that $\sigma \sim N^{1/3}$ [1,24].

A very interesting feature emerges from the behavior of σ as a function of P_{ba} for a fixed mean radius of the active zone, as shown in the inset of Fig. 4. The active zone width is a convex function of P_{ba} with a maximum at $P_{ba}=1/2$, which explains the lacunarity dependence on P_{ba}. The onset of this qualitative behavior can be understood through an analysis of the screening properties of the clusters: for $P_{ba} \gtrsim 0$, the patterns have large grooves and the ballistic trajectories can reach the inner regions of the cluster forbidden for random walks. Thus, the screening is reduced in relation to the original DLA model and, consequently, the active zone is enlarged. As P_{ba} increases, more particles break the screening enlarging the active zone. However, if too many particles arrive at the inner regions of the clusters, the size of their grooves and, consequently, their active zones are reduced. Therefore, the convexity of σ versus P_{ba} was elucidated. Intriguingly, this change of behavior seems to occur when the number of DLA and BA particles are equal, but we cannot provide a rigorous justification besides the numerical evidence.

One of the most complex features of DLA clusters is their multiscaling structures [5,16,17], which were recently analyzed by Mandelbrot *et al.* at the light of the angular gap distributions of the clusters [5]. They found that the angular and radial distributions of mass scale with the same exponent $D \approx 1.71$ only for very small angular gaps. This happens for asymptotically large clusters ($M \approx 10^8$) when the number of main branches increases leading to a more uniform space fulfillment. From Fig. 2, one can see that angular gap distributions vary with the parameter P_{ba}. Therefore, an angular scaling analysis becomes necessary in order to obtain a more elaborate characterization of the model. For this task, we
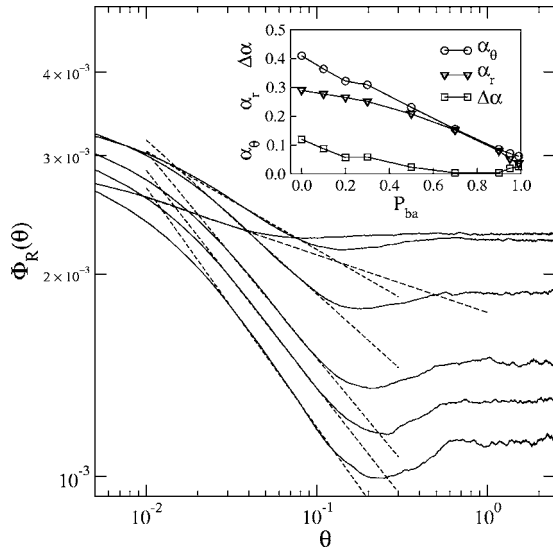
FIG. 5. Two-point angular correlation functions evaluated at R $=300$ for several values of P_{ba}: 0.1, 0.2, 0.3, 0.5, 0.7, and 0.9 from the bottom to the top, respectively. The dashed lines correspond to the power law fits for small θ. In the inset, the angular and radial correlation function exponents are compared. The size of the clusters is 5000×5000 and Φ_R was evaluated using $R=300$ and δR $=15$. The averages were done over $N=10^3$ independent samples.

FIG. 6. Behavior of the minima presented in angular correlation functions for distinct probabilities P_{ba}. The dashed line is a power-law fit corresponding to an exponent $\vartheta \approx 0.45$. Data in the range $P_{ba} \in [0.1, 0.95]$ are shown. The insets show the linear plots of Φ_R for the regions near the minima for $P_{ba}=0.7$ (bottom) and P_{ba} $=0.9$ (top). The solid lines are the cubic fits used to determine the positions of the minima.

followed the work of Meakin and Vicsek [15], in which they analyzed the angular correlations of the DLA model using the following procedure. A narrow circular shell of radius R and width $\delta R \ll R$ centered at the origin is divided in K identical sectors of area $R \delta\theta \delta R$, where $\delta\theta = 2\pi/K$. For a box centered at the polar coordinates (R, ϕ), the quantity $\rho_R(\phi)$ $= \kappa$ is defined, where κ is the number of particles within this box. The two-point angular correlation function is given by

$$\Phi_R(\theta) = \frac{1}{N} \sum_{n=0}^{K/2} \rho_R(\theta + n\delta\theta)\rho_R(n\delta\theta). \quad (11)$$

The exponent obtained for the relatively small DLA clusters ($\sim 10^5$) using this procedure was $\alpha_\theta \approx 0.41$, which is definitely different from $\alpha_r \approx 0.29$.

Figure 5 illustrates the angular correlation functions evaluated at $R=300$ for distinct P_{ba} values. In all curves, $\Phi_R(\theta)$ decays as a power law for small angles followed by a global minimum and reaches a constant value for large angles. This behavior qualitatively reproduces the finds by Meakin and Vicsek [15], but the power law exponents decay with P_{ba} as illustrated in the inset of Fig. 5, in which α_θ and α_r, as well as the difference between them, $\Delta\alpha$, are plotted as functions of P_{ba}. The exponent α_r was determined using the relation $\alpha_r = 2 - d_f$, where $\overline{d_f}$ is the mean fractal dimension obtained through the mass-radius and radius of gyration methods [Fig. 3(b)]. The difference $\Delta\alpha \approx 0.12$ observed for the DLA model decreases with P_{ba}. The minima of the curves are interesting quantities since they represent estimates of the half angular separation between two consecutive branches, the gaps studied by Mandelbrot et al. [5]. The minima position shift to small angles and become less evi-
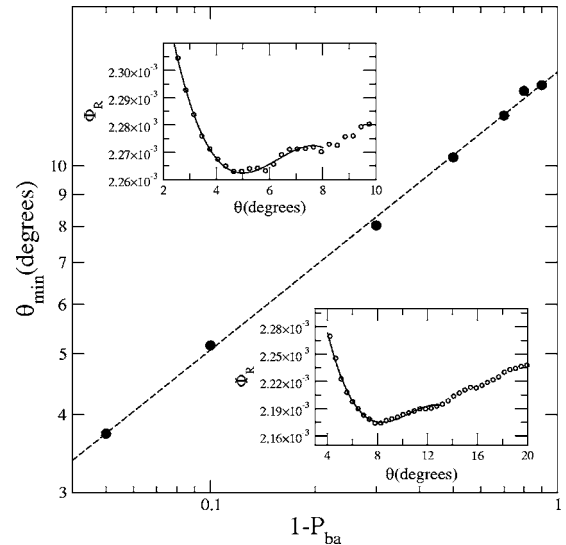
dent with increasing P_{ba}. Indeed, the extrapolation of minimum positions suggests that their values vanish at $P_{ba}=1$ following a power law $\theta_{min} \sim (1 - P_{ba})^\vartheta$, where $\vartheta \approx 0.45$, as shown in Fig. 6. The minima were determined using a cubic fit around their positions, as indicated in the insets of Fig. 6. This power law relation means that the angular gaps are present, even that small, for any $P_{ba} \neq 1$. However, one can resolve from the inset of Fig. 5 the difference $\Delta\alpha$ vanishing for $P_{ba} \gtrsim 0.5$. This behavior of $\Delta\alpha$ agrees with the concluding claim of Mandelbrot et al. [5] concerning the asymptotic scaling of ordinary off-lattice DLA clusters. Indeed, in our model the gaps are reduced with increasing P_{ba} and, consequently, we observed the same result of Ref. [5], but without considering simulations with more than 10^8 particles.

IV. SUMMARY

In this work, we analyzed an aggregation model in which two kinds of particles are considered: a given fraction following Brownian motions and the remaining following ballistic trajectories. The model, which includes diffusion-limited aggregation (DLA) and ballistic aggregation (BA) models as limit cases, is controlled by a probability P_{ba} that corresponds to the fraction of BA particles that constitutes the aggregate. Large-scale simulations and careful statistical sampling were used to characterize the radial and angular scaling of off-lattice aggregates. Specifically, we measured the fractal dimension d_f, the lacunarity, the width of active (growing) zone σ, and the angular correlation function Φ_R of clusters grown for distinct P_{ba} values.

The fractal dimension d_f continuously increases from d_f $=1.715 \pm 0.004$ for $P_{ba}=0$ (DLA fractal dimension) to $d_f \approx 2$

(BA fractal dimension). However, the lacunarity and the width of the active zone for a fixed radius are convex functions of the probability P_{ba} with maxima at $P_{ba} \approx 1/2$. The convexity of the lacunarity is directly related to the convexity of the active zone width, which in turn was explained by the screening impairing the wandering particles to reach the inner regions of the clusters.

The angular correlation function $\Phi_R(\theta)$ evaluated at $R = 300$ exhibits a power law decay for small angles with an exponent that is a decreasing function of P_{ba}. The difference between angular and radial exponents observed for the original off-lattice DLA model [15] was found, but it rapidly vanishes for $P_{ba} > 1/2$. Also, the curves Φ_R versus θ exhibit global minima representing the half angular separations between two consecutive branches. The simulations show that the position of the minima vanishes as $P_{ba} \rightarrow 1$ following a power law $\theta_{min} \sim (1 - P_{ba})^\vartheta$ with $\vartheta \approx 0.45$. These results indicate that the patterns are asymptotically homogeneous when $P_{ba} \rightarrow 1$. In summary, in this work we show how the scaling properties of the aggregates can be controled by varying the concentration of the kinds of wandering particles involved in the growth process. Finally, it is important to emphasize that these results are in agreement with the angular gap distribution analysis performed by Mandelbrot *et al.* [5], in which they found that the original DLA clusters exhibit the same asymptotic angular and radial scaling.

[1] P. Meakin, *Fractals, Scaling, and Growth Far from Equilibrium* (Cambridge University Press, Cambridge, 1998).

[2] L. M. Sander, Contemp. Phys. **41**, 203 (2000).

[3] T. A. Witten and L. M. Sander, Phys. Rev. Lett. **47**, 1400 (1981).

[4] E. Somfai, L. M. Sander, and R. C. Ball, Phys. Rev. Lett. **83**, 5523 (2000).

[5] B. B. Mandelbrot, B. Kol, and A. Aharony, Phys. Rev. Lett. **88**, 055501 (2002).

[6] M. H. Jensen, J. Mathiesen, and I. Procaccia, Phys. Rev. E **67**, 042402 (2003).

[7] N. R. Goold, E. Somfai, and R. C. Ball, Phys. Rev. E **72**, 031403 (2005).

[8] M. J. Vold, J. Colloid Sci. **18**, 684 (1963).

[9] S. Liang and L. P. Kadanoff, Phys. Rev. A **31**, 2628 (1985).

[10] S. C. Ferreira, Jr., S. G. Alves, A. F. Brito, and J. G. Moreira, Phys. Rev. E **71**, 051402 (2005).

[11] M. Castro, R. Cuerno, A. Sánches, and F. Domígues-Adame, Phys. Rev. E **62**, 161 (2000).

[12] Y. Kim, K. R. Choi, and H. Pak, Phys. Rev. A **45**, 5805 (1992).

[13] P. Meakin, Phys. Rev. B **28**, 5221 (1983).

[14] T. Nagatani, Phys. Rev. A **39**, 438 (1989).

[15] P. Meakin and T. Vicsek, Phys. Rev. A **32**, 685 (1985).

[16] B. B. Mandelbrot, A. Vespignani, and H. Kaufman, Europhys. Lett. **32**, 199 (1995).

[17] E. Somfai, R. C. Ball, N. E. Bowler, and L. M. Sander, Physica A **325**, 19 (2003).

[18] S. Tolman and P. Meakin, Phys. Rev. A **40**, 428 (1989).

[19] C. Tang and S. Liang, Phys. Rev. Lett. **71**, 2769 (1993).

[20] J. Yu and J. G. Amar, Phys. Rev. E **66**, 021603 (2002).

[21] R. C. Ball and R. M. Brady, J. Phys. A **18**, L809 (1985).

[22] C. Amitrano, A. Coniglio, P. Meakin, and M. Zannetti, Phys. Rev. B **44**, 4974 (1991).

[23] M. Kardar, G. Parisi, and Y. C. Zhang, Phys. Rev. Lett. **56**, 889 (1986).

[24] A.-L. Barabasi and E. H. Stanley, *Fractal Concepts on Surface Growth* (Cambridge University Press, Cambridge, 1995).